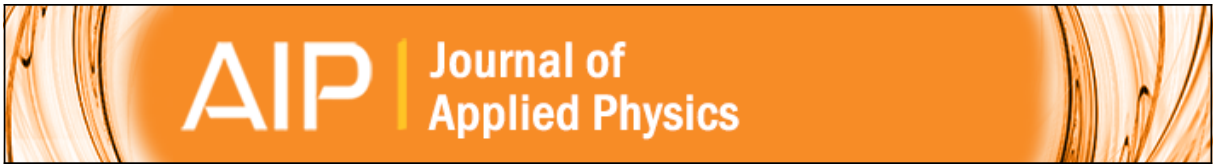

Electron transport properties in Nb and NbN cluster-assembled films produced by a plasma–gas–condensation cluster source

T. Hihara, Y. Yamada, M. Katoh, D. L. Peng, and K. Sumiyama

Citation: Journal of Applied Physics **94**, 7594 (2003); doi: 10.1063/1.1629152
View online: http://dx.doi.org/10.1063/1.1629152
View Table of Contents: http://scitation.aip.org/content/aip/journal/jap/94/12?ver=pdfcov
Published by the AIP Publishing

Electron transport properties in Nb and NbN cluster-assembled films produced by a plasma–gas–condensation cluster source

T. Hihara,[a] Y. Yamada, M. Katoh, D. L. Peng, and K. Sumiyama
Department of Materials Science and Engineering, Nagoya Institute of Technology, Nagoya 466-8555, Japan

(Received 19 May 2003; accepted 6 October 2003)

Nb and NbN cluster-assembled films were produced by a plasma–gas–condensation cluster deposition apparatus and examined by transmission electron microscopy, electrical resistivity, and ultraviolet photoemission spectroscopy. The electron diffraction patterns of the Nb and NbN clusters displayed body-centered-cubic and NaCl-type diffraction rings, respectively. The electrical sheet resistance, $R_{\square}$, of both Nb and NbN cluster-assembled films, however, showed no superconductivity down to 2 K. We found a linear relation in the log $R_{\square}$ versus $T^{-1/4}$ plot for the Nb cluster assembly, suggesting an electron localization effect. For the NbN cluster-assembly, on the other hand, $R_{\square}$ showed a semiconductor type temperature dependence, which is consistent with the valence electron spectra. © *2003 American Institute of Physics.* [DOI: 10.1063/1.1629152]

I. INTRODUCTION

Small particle and/or cluster assemblies are promising to obtain nanoscale structure controlled materials, which reveal unique physical and chemical properties owed to their low dimensionality.[1–6] In order to obtain size-selected clusters as building blocks, we have constructed a plasma–gas–condensation (PGC)-type cluster deposition apparatus,[6–9] which is a combination of sputter vaporization and inert gas–condensation techniques, and is applicable to vaporizing refractory metals. The clusters formed in a source region are extracted through a nozzle into a better vacuum chamber in order to prevent further cluster growth and minimize their oxidation. Hence, we have obtained clusters, whose mean sizes are controllable between 3 and 13 nm in diameter.

Superconductivity in the nanometer-sized clusters has been actively discussed in terms of their finite size and surface effects.[10–12] The superconducting transition temperature T_c of the clusters as a function of their size d has been studied both theoretically and experimentally. For weak-coupling superconductors, T_c is an increasing function of $1/d$ as investigated in Al and In cluster assembles, whereas, it is in dependent of d in strong-coupling Pb clusters down to at least $d=5$ nm.[11] Phonon softening near the surface well explains the size dependence of T_c in weak- and intermediate-coupling systems but does not in the strong-coupled Pb clusters.[10]

The surface of nanometric clusters used to be structurally disordered and oppositely contributes to the transport property:[13–15] In heterogeneous superconducting films an electron localization effect induces a metal–insulator transition. The aim of this work is to comprehend the surface effect in small superconducting clusters. In this context, we have prepared Nb and NbN cluster-assembled films by the other PGC-type cluster deposition apparatus in which clusters can be deposited on substrates under an ultrahigh-vacuum condition.[16] In this article we describe the structural and electronic properties of the Nb and NbN cluster-assembled films fabricated with this apparatus.

II. EXPERIMENT

Nb clusters were synthesized by a PGC apparatus, whose details have been described elsewhere.[16] A continuous Ar gas stream was injected through the 0.3 mm gap between the shield cover and the target in order to avoid the accumulation of formed particles that cause the abnormal discharge and the short circuit during the glow discharge operation. The metal vapors were generated from a Nb target by dc magnetron sputtering. Clusters nucleate in a high-pressure Ar gas atmosphere (0.2–0.7 kPa) and grow in the space between the target and the nozzle (the growth region), whose length, L_g can be varied by moving the sputtering source back and forth. He gas was also introduced into the sputtering chamber from the back side of the source. The cluster beam was extracted through the nozzle of 5 mm in diameter by differential pumping and further collimated by the three skimmers. For transmission electron microscope (TEM) observation, a microgrid, which is a carbon-coated colodion film supported by a Cu grid, was used as a substrate. The samples were exposed in air for transportation and observed with a cold cathode-field emission-type transmission electron microscope, operating at 200 kV. The TEM images were taken as digitized data with a slow-scan charge coupled device camera installed in the electron microscope. Using the conventional four-probe method, the sheet resistance was measured at a constant current between 2 and 300 K. For *in situ* characterization of those cluster-assembled films, an ultraviolet-photoemission spectrometer was connected to the cluster deposition apparatus. For this purpose, we constructed another cluster deposition chamber whose vacuum condition is about 10^{-10} Torr. The measurements were carried out at 25 K with a He gas–discharge lamp producing photons of 21.2 eV (He I).

[a]Electronic mail: hihara@mse.nitech.ac.jp

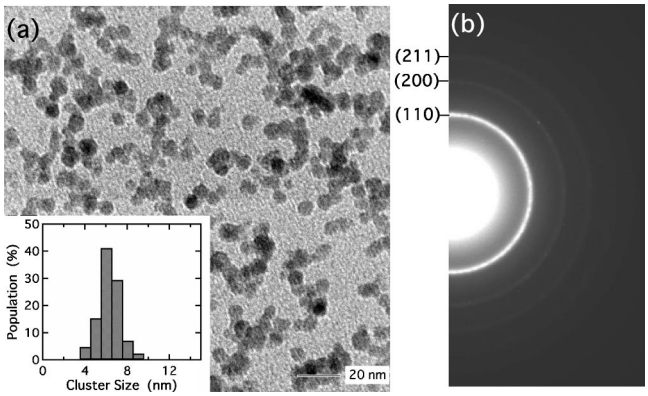

FIG. 1. (a) A BF-TEM image and (b) the ED pattern of the Nb clusters obtained with $P_W=300$ W, $L_g=120$ mm, $V_{\mathrm{Ar}}=2.3\times10^{-4}$, and $V_{\mathrm{He}}=4.5\times10^{-4}$ mol/s.

III. RESULTS

A. Nb cluster assembly

Figure 1(a) shows a typical bright-field (BF) TEM image of the Nb clusters prepared under the following conditions: $P_w=300$ W, $L_g=120$ mm, $V_{\mathrm{Ar}}=2.3\times10^{-4}$ [300 standard cubic centimeter per minute (sccm)], and $V_{\mathrm{He}}=4.5\times10^{-4}$ mol/s (600 sccm). Here, P_w is the sputtering power and V_{Ar} and V_{He} are the gas flow rates of Ar and He, respectively. The size distribution histogram estimated from the deposited area of 0.036 μm^2 ranges from 4 to 9 nm for the Nb clusters with the mean size of 6.3 nm as shown in the inset of Fig. 1(a). The corresponding electron diffraction (ED) pattern is shown in Fig. 1(b). The ED pattern of these Nb clusters displays one set of diffraction rings being ascribed to a body-centered-cubic (bcc) structure with the lattice parameter of 0.330 ± 0.005 nm. This is consistent with the reported value of 0.3307 nm of the bulk specimen, whereas we could not detect any diffraction spots corresponding to the niobium oxide.

Figure 2(a) shows the electrical sheet resistance $R_{\square}(T)$ as a function of temperature T for the Nb cluster-assembled film. Although the superconducting transition temperature of the bulk Nb specimen is 9.5 K, the temperature dependence of $R_{\square}$ reveals no superconducting transition between 2 and 300 K but a semiconductorlike behavior: $R_{\square}(T)$ increases gradually as T decreases and it shows an abrupt increase below 30 K.

For magnetic measurement, Nb clusters were deposited on a Si wafer with Au buffer and cover layers in order to minimize their oxidation. We measured magnetic susceptibility using a superconducting quantum interference device magnetometer down to 1.8 K, and could not detect a Meissner effect. The possible explanation for this result is that the cluster size is smaller than the penetration depth of an applied magnetic field (10 Oe) or the Nb cluster-assembled film exhibits no superconductivity within the measured temperature range.

In strongly disordered films, the electrical conduction is dominated by the electron hopping between localized sites, and the temperature dependence of the resistivity $\rho(T)$ is described as $\rho=\rho_0\exp[-(T/T_0)^{\alpha}]$, where ρ_0, T_0, and α are

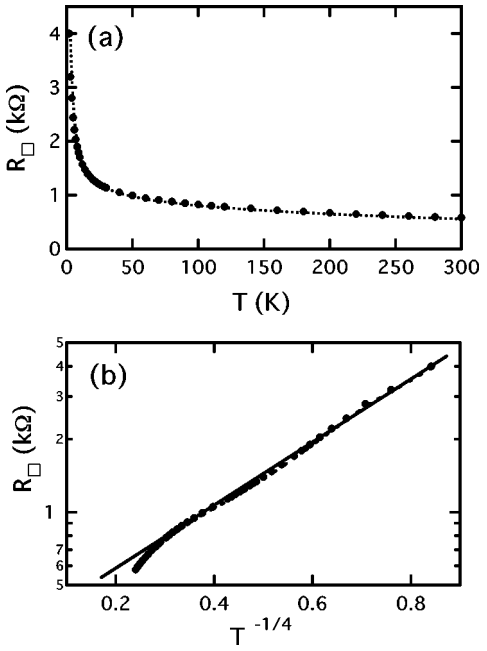

FIG. 2. (a) Temperature dependence of the electrical resistance $R_{\square}(T)$ and (b) the logarithmic resistance, $\log R_{\square}(T)$, as a function $T^{-1/4}$ for Nb cluster-assembled film.

constants which depend on the degree of disorder, interactions, and dimensionality of the system.[12,13] It has been reported that α varies from 1 for the simply activated hopping across a constant barrier (Arrhenius type), 0.75 for collective variable range hopping, 0.5 for hopping dominated by Coulomb interaction, and $1/(D+1)$ for Mott variable range hopping, where D is the dimension of system.[14] It is also notable that in the weak localization regime the conductivity $\sigma(T)$ shows a logarithmic temperature dependence, $\sigma=\sigma_0+(e^2p/2\hbar\pi^2)\ln(T_0/T)$, where p is a coefficient determined by the electron scattering mechanism.[13] As shown in Fig. 2(b), we find a linear relation in the $\log R_{\square}$ on $T^{1/4}$ plot between 2 and 30 K for the present Nb cluster-assembled film.

B. NbN cluster assembly

Niobium nitride is a refractory material with a bulk superconducting transition temperature of about 16 K.[17] Thin films of NbN, typically deposited by reactive sputtering methods in an argon/nitrogen plasma, are also studied for applications. Figures 3(a) and 3(b) show a typical BF-TEM image of the NbN clusters obtained at N_2 gas flow rates, $V_{\mathrm{N_2}}=1.5\times10^{-6}$ mol/s (2.0 sccm) and the corresponding ED pattern, respectively. The experimental conditions were as follows: $L_g=120$ mm, $V_{\mathrm{Ar}}=2.3\times10^{-4}$ mol/s (300 sccm), $V_{\mathrm{He}}=4.5\times10^{-4}$ mol/s (600 sccm), and $P_w=300$ W. At $V_{\mathrm{N_2}}=1.5\times10^{-6}$ mol/s, we obtained almost spherical clusters whose sizes are distributed between 5 and 10 nm in diameter with the mean size of 7.6 nm. The ED pattern of these NbN cluster-assembly displays one set of diffraction rings being ascribed to a NaCl-type structure with the lattice parameter of 0.440 ± 0.005 nm. This is consistent with the reported value of δ-NbN (0.4389 nm) with a B1(NaCl-type) structure.

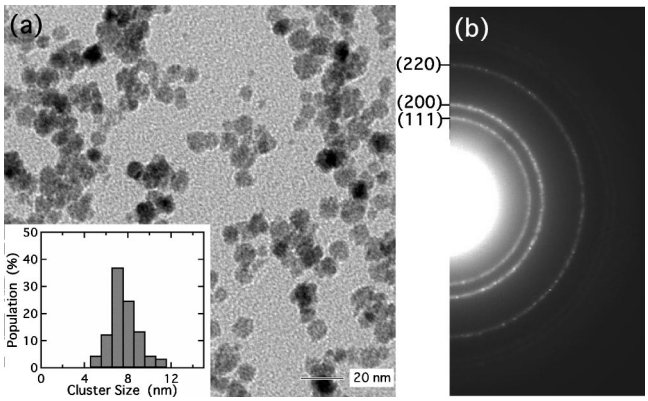

FIG. 3. (a) A BF-TEM image and (b) the ED pattern of the NbN clusters obtained with $P_W=300$ W, $L_g=120$ mm, $V_{N_2}=1.5\times10^{-6}$, $V_{Ar}=2.3\times10^{-4}$, and $V_{He}=4.5\times10^{-4}$ mol/s.

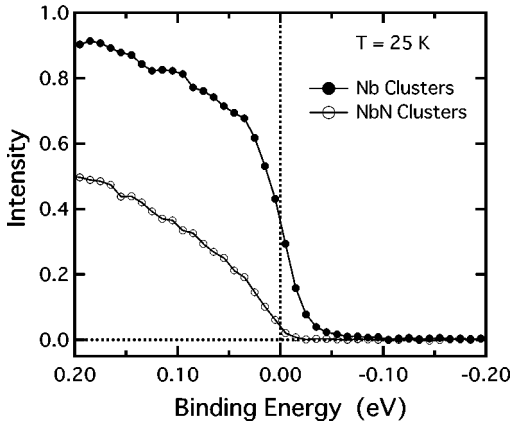

FIG. 5. Photoemission spectra near Fermi level obtained with He I excitation for Nb and NbN cluster-assembled films.

Figure 4(a) shows $R_\square$ as a function of T for the NbN cluster-assembled film. The temperature dependence of $R_\square$ also reveals no superconducting transition down to 2 K: $R_\square(T)$ increases gradually as T decreases and it also shows a dramatical increase below 30 K. We obtained no linear dependence in the $\log R_\square$ versus $T^{-\alpha}$ plot with $\alpha<1$. As shown in Fig. 4(b), we replotted $R_\square(T)$ in a form of $\log R_\square$ versus $1/T$ and obtained a good linear relationship at low temperatures. The estimated activation energy from Fig. 4(b) is about 45 meV for $T<30$ K.

Figure 5 shows the valence electron spectra of the present Nb and NbN cluster-assembled films. As shown here, the photoemission intensity from the Nb clusters sharply drops at zero-binding energy, indicating that the Nb cluster assembly has a metallic band structure. For the NbN clusters, on the other hand, the marked reduction in the density of states at the Fermi level indicates that the valence-band edge is shifted to a lower binding energy.

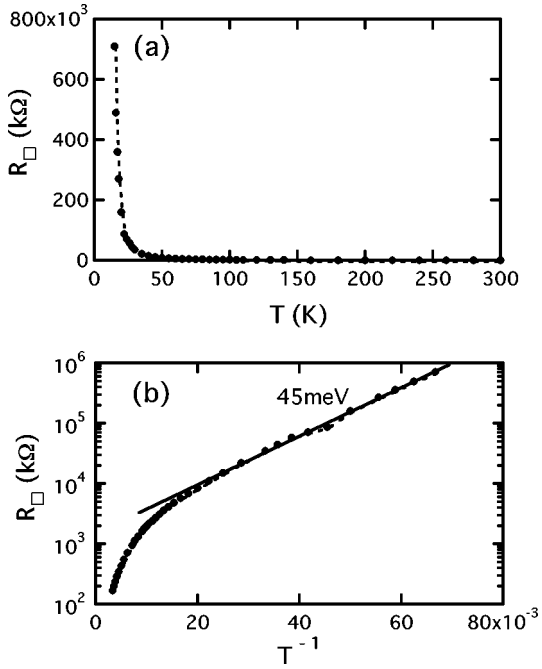

FIG. 4. (a) Temperature dependence of the electrical resistance $R_\square(T)$ and (b) the logarithmic resistance, $\log R_\square(T)$, as a function T^{-1} for NbN cluster-assembled film.

IV. DISCUSSION

We have observed that the Nb cluster-assembled film deposited in an ultrahigh-vacuum cluster deposition apparatus has a bcc structure with the same lattice constant as the bulk counterpart, and a metallic valence-band structure. It does not show a superconducting behavior down to 2 K. The ED pattern of the Nb clusters indicates no diffraction spots corresponding to niobium oxides. However, those results do not exclude the surface oxidization that cannot be detected by the electron diffraction technique.

In homogeneous superconducting films, the resistivities are smoothly turned to the superconducting states and the transition temperatures are decreased from the bulk value by decreasing the film thickness.[14,15] At the insulator–superconductor transition, the localization length of electrons and the superconducting coherent length become comparable. When the film is thinner, the Cooper pairs are finally destroyed due to the disorder and/or the low dimensionality, and then hopping conduction and/or percolation dominate the electron transport properties. In heterogeneous superconducting films, on the other hand, the individual grains become superconducting below the bulk transition temperature, where the Josephson coupling energy E_J and charging energy E_c compete with each other. There are no free electrons in these systems because of Cooper pairing, and the conduction is attributed to the tunneling of Cooper pairs between superconducting grains. Since $E_c>E_J$ for the system with large intergrain capacitance, the tunneling conduction is prevented, leading to the localization of Cooper pairs.

For our Nb cluster-assembled film, it is still open to question whether Cooper pairs disappear and the Fermion localization effect appears, or the boson state is still kept in the individual Nb clusters and the transportation is dominated by Cooper pairs hopping. As shown in Fig. 2(b), the Mott variable range hopping in a three-dimensional system is a good representation for the electron transportation. This result indicates that the localization length related to the elec-

tron elastic mean-free path is limited within the Nb cluster and/or shorter than the superconducting coherence length. For the NbN cluster-assembled film, on the other hand, $R_{\square}$ shows a semiconductor-type temperature dependence, which is consistent with the valence electron spectrum of the NbN cluster assembly. This behavior may reflect the off stoichiometry of NbN and/or enhancement of disordered interfaces between the NbN clusters.

V. CONCLUSION

Nb and NbN cluster-assembled films were prepared by a PGC cluster deposition apparatus and examined by transmission electron microscopy, electrical resistivity, and ultraviolet photoemission spectroscopy. The electrical resistivity of both Nb and NbN cluster assemblies show no superconductivity down to 2 K against their bulk specimens. We found a linear dependence of $\log R_{\square}$ versus $T^{1/4}$ in the Nb cluster assembly, suggesting that Mott variable range hopping is dominant. For the NbN cluster-assembled film, on the other hand, $R_{\square}$ shows a semiconductor-type temperature dependence, which is consistent with the valence electron spectra of NbN cluster assembly. In order to understand the detailed electron transportation in the superconductor cluster-assembled systems, we are now carrying out the conductivity measurements with different cluster sizes. These results will be published elsewhere.

ACKNOWLEDGMENTS

This work has been supported by a Core Research for Evolutional Science and Technology (CREST) of Japan Science and Technology Corporation (JST), a Grant-in-Aid for scientific research project of ''Intellectual Clusters,'' and a Grant-in-Aid for General Scientific Research (Grant No. 13750609) given by the Ministry of Education, Culture, Sports, Science, and Technology of Japan. One of the authors (D.-L.P.) appreciates the financial support from Japan Society for the Promotion of Science (JSPS). The authors appreciate the experimental assistance of D. Matsuda.

[1] H. Gleiter, Prog. Mater. Sci. **33**, 223 (1989).
[2] R. Uyeda, Prog. Mater. Sci. **35**, 1 (1991).
[3] P. Melinon, V. Paillard, V. Dupuis, A. Perez, P. Jensen, A. Hoareau, J. P. Perez, J. Tuaillon, M. Broyer, J. L. Vialle, M. Pellarin, B. Baguenard, and J. Lerme, Int. J. Mod. Phys. B **9**, 339 (1995).
[4] H. Haberland, *Clusters of Atoms and Molecules I and II* (Springer, Berlin, 1995).
[5] W. A. de Heer, Rev. Mod. Phys. **65**, 611 (1993).
[6] W. Eberhardt, Surf. Sci. **500**, 242 (2002).
[7] S. Yamamuro, K. Sumiyama, M. Sakurai, and K. Suzuki, Supramol. Sci. **5**, 239 (1998).
[8] H. Haberland, M. Karrais, M. Mall, and Y. Thurner, J. Vac. Sci. Technol. A **10**, 3266 (1992).
[9] H. Haberland, M. Mall, M. Moseler, Y. Qiang, T. Reiners, and Y. Thurner, J. Vac. Sci. Technol. A **12**, 2925 (1994).
[10] B. Abeles, Appl. Solid State Sci. **6**, 64 (1976).
[11] S. Matsuo, H. Sugiura, and S. Noguchi, J. Low Temp. Phys. **15**, 481 (1974).
[12] C. R. Leavens and E. W. Fenton, Phys. Rev. B **24**, 5086 (1981).
[13] P. A. Lee and T. V. Ramakrishnan, Rev. Mod. Phys. **57**, 287 (1985).
[14] N. Markovió, C. Christiansen, D. E. Grupp, A. M. Mack, G. Martinez-Arizala, and A. M. Goldman, Phys. Rev. B **62**, 2195 (2000).
[15] G. Sambandamurthy, K. Das Gupta, and N. Chandrasekhar, Phys. Rev. B **64**, 014506 (2001).
[16] T. Hihara, K. Sumiyama, M. Sakurai, R. Czajka, and A. Kasuya, Proc. Int. Symp. on Cluster Assembled Mater. IPAP Conf. Series **3**, 12 (2001).
[17] G. Lamura, J.-C. Villégier, A. Gauzzi, J. Le Cochec, J.-Y. Laval, B. Plaçais, N. Hadacek, and J. Bok, Phys. Rev. B **65**, 104507 (2002).